Fabrication and Properties of Degradable Poly(amino acid)/Nano Hydroxyapatite Bioactive Composite

Zhitong Zhao,[1] Wenpeng Shan,[2] Yunfei Zhang,[1] Xiangde Li,[2] Jian Ma,[3] Yonggang Yan[1]

[1]*School of Physical Science and Technology, Sichuan University, Chengdu 610064, China*
[2]*Key Laboratory for Ultrafine Materials of Ministry of Education, East China University of Science and Technology, Shanghai 200237, People's Republic of China*
[3]*Hospital of Stomatology, Tongji University, Shanghai 200072, China*

Received 19 July 2011; accepted 7 October 2011
DOI 10.1002/app.36355
Published online 28 January 2012 in Wiley Online Library (wileyonlinelibrary.com).

ABSTRACT: Poly(amino acid)/nano hydroxyapatite (PAA/n-HA) bioactive composite was prepared by *in situ* melting polymerization. The composition, structure and morphology as well as glass transition temperature (T_g), dynamic mechanical properties of the PAA/n-HA composite were characterized by infrared spectrometer, X-ray diffractometer, X-ray photoelectron spectroscopy, scanning electron microscope, differential scanning calorimeter, and dynamic mechanical analyzer. The results indicated that the n-HA particles were uniformly distributed into PAA matrix and some interactions were found at the interface between PAA and n-HA, and the crystallinity of PAA in the composite decreased with the increase of n-HA content. The T_g and storage modulus of the composite increased with increasing n-HA content, demonstrating that the n-HA content had obvious effects on the crystallization kinetic parameters and thermo properties of the PAA/n-HA composite. In addition, the n-HA amount had evident effects on the degradation of the PAA/n-HA composite in phosphate buffered saline (PBS), and the weight loss ratio of the composite decreased with the increase with n-HA content. The pH value of the medium was stable around 7.40 after the composite immersion into PBS for 8 weeks. © 2012 Wiley Periodicals, Inc. J Appl Polym Sci 125: 2502–2509, 2012

Key words: poly(amino acid); nanocomposites; glass transition; dynamic mechanical properties; degradation

INTRODUCTION

In the past few years, Ca–P bioceramic has been widely applied for bone replacement due to its excellent biocompatibility and bioactivity.[1,2] Amongst the Ca–P family members, hydroxyapatite (HA) with excellent bioactivity is the most prominent and has gained much attention because it has similarity to bone apatite in chemical composition and crystal structure, and can form bone bonding with bone tissue. However, HA ceramic is fragile and will crack under the stress that limits its application in the load-bearing bone repair.[3–5]

Biodegradable polymer has been found a wide range of biomedical applications, such as sutures, bone fracture fixation devices, and tissue engineering scaffolds due to their degradability and good biocompatibility. But polymer still can not ideally meet the requirements in bone repair because of its soft character and lacking of bone-bonding bioactivity.[6,7] To improve the bioactivity of polymer, more attention is paid to fabricate polymer/HA bioactive composite. These bioactive composites included poly(lactic acid)/HA,[8–10] poly(glycolic acid)/HA, the co-polymer poly(lactide-*co*-glycolide)/HA,[11,12] and poly(ε-caprolactone)/HA[13,14] since they have the properties of osteoconductivity and degradability. However, some of these polymers undergo a bulk erosion process so that they can cause scaffolds to fail prematurely. In addition, these polymers abrupt release of acidic degradation products that can cause inflammatory responses.[6,15]

The poly(amino acid) polymer is considered to be promising biomedical materials because of its polypeptide backbone, which has the potential to be degraded into amino acid monomers in biological environments.[16] Poly(amino acid) polymer has been reported in the past years, and has been applied in drug controlled release, absorbable suture, and artificial skin.[17,18] However, poly(amino acid) copolymer/nano-hydroxyapatite (PAA/n-HA) bioactive composites are seldom concerned in bone tissue repair. In this study, the PAA polymer was obtained

Correspondence to: Y. Yan (biomater2006@yahoo.com.cn or yan_yonggang@vip.163.com).

Contract grant sponsor: National Key Technology R&D Program in the 11th Five Year Plan of China; contract grant number: 2007BAE12B00.
Contract grant sponsor: Nano special program of Science and Technology Development of Shanghai; contract grant number: 1052nm06600.
Contract grant sponsor: Key Medical Program of Science and Technology Development of Shanghai; contract grant number: 09411954900.

by the polymerization of 6-aminohexanoic acid, phenylalanine, lysine, hydroxyproline and proline. In previous work, a series of poly(amino acid) copolymers and their composites have been prepared,[19] but the relative work analyzing the dynamic mechanical properties has hardly been addressed. Therefore, in this study, the dynamic mechanical properties as well as T_g of the PAA/n-HA composite were detected by dynamic mechanical analyzer (DMA) and differential scanning calorimeter (DSC), and the *in vitro* degradation of PAA/n-HA composite in phosphate buffered saline (PBS) was investigated.

EXPERIMENTAL

Preparation and characterization of PAA/n-HA composite

The PAA/n-HA composites containing 10 wt %, 20 wt %, 30 wt % of n-HA named PAA/n-HA 10, PAA/n-HA 20, and PAA/n-HA 30 were prepared using *in situ* melting polycondensation.[19] Briefly, 104.9 g 6-aminohexanoic acid, 3.3 g phenylalanine, 4.4 g lysine, 13.1 g hydroxyproline, and 5.8 g proline were added into the three-necked flask, and 0.5 mL phosphorous acid was added as catalyst. To avoid oxidation, the polymerization process proceeded under a continuous flow of nitrogen. The mixture with strong stirring was kept at 180°C until the water was evaporated, followed by melting at 210°C, and then the mixture was kept at 220°C for 1 h. Different amount of n-HA powder was added into the three necked-flask and then the mixture was kept at 230°C for another 1 h. After reaction, the product was kept under a nitrogen environment until it was cooled down to room temperature. The PAA/n-HA composites with different content were obtained. The poly(amino acid) was prepared as a control using the same method. Fourier transforms infrared (FTIR) spectroscopy spectra were collected using a Perkin–Elmer 6000 FTIR spectrometer (Nicolet Perkin–Elmer Co., Waltham, Massachusetts, USA). A wide-angle XRD patterns of all the samples were recorded using a X-ray diffractometer (X'Pertpro-MPD, PANalytical Co. Almelo, Netherlands) with Cu Kα radiation ($\lambda = 1.54$ Å). X-ray photoelectron spectroscopy (XPS) was carried out with a XSAM 800 (Kratos) Instrument. The morphology of the PAA/n-HA composite was observed by scanning electron microscopy (SEM, JEOL JSM 5600LV, Mitaka, Tokyo, Japan) at 20 kV.

Thermal and dynamic mechanical properties

The glass transition temperature of the PAA/n-HA composites and PAA were determined by a differential scanning calorimeter (DSC Q200, TA Instruments, Santa Clara, California, USA). First, the samples were heated from 20 to 210°C, followed by staying at 210°C for 5 min to eliminate the thermal history, and then cooled down from 210 to 20°C. Finally, the samples were heated from 20 to 210°C. Every step with a rate of 10°C/min proceeded under the nitrogen flow. The second heating data was collected to determine the T_g. Weight of all the samples were from 4 to 6 mg. Dynamic mechanical properties of the PAA/n-HA composites and PAA were determined by DMA analyzer Q800 (TA Instruments, Santa Clara, California, USA). The measurements were performed in three-point bending model at frequency of 1 HZ, and the temperature was range from 20 to 110°C with a ramp of 3°C/min. The storage modulus of the specimens with the size of $40 \times 10 \times 4$ mm^3 was tested.

In vitro degradation of PAA/n-HA composite

To evaluate the *in vitro* degradation of the PAA/n-HA composites (PAA as a control), the samples were cut into cakes with the size of $10 \times 10 \times 4$ mm^3, then the specimens were soaked in PBS (pH 7.4) at 37.0°C in shaking water bath with a weight-to-volume ratio of 1/30 g/mL. After different time point, the samples were removed from the PBS, cleaned with deionized water, dried at 70°C for 4–6 h. The samples were then re-immersed into a fresh PBS at the same weight-to-volume ratio followed by continuous shaking. This process was repeated over a period of 8 weeks for all samples. The weight loss ratio of each sample at different time point was calculated as percentage of the initial weight. Three samples of each kind of scaffold were tested, and the average value was present. The pH of the PBS medium after the samples soaking was recorded at each time point.

RESULTS AND DISCUSSION

IR analysis

The IR patterns of PAA, n-HA, and PAA/n-HA 30 composite were shown in Figure 1. The absorption peak at 3340 cm^{-1} in Figure 1(a) represented the stretching vibration of N—H of PAA. The peaks at 2943 cm^{-1}, 2866 cm^{-1} were attributed to the characteristic peaks of methyl and methylene groups. The peak at 1640 cm^{-1} belonged to the stretching vibrations of carbonyl groups in PAA, caused by the interaction between —NH_2 group and —COOH group. The band around 1542 cm^{-1} represented the bending vibrations of hydrogen–nitrogen. Moreover, it could be not found that the characteristic peak of carboxyl at 1740 cm^{-1} in PAA and PAA/n-HA composite.

The peak at 3437 cm^{-1}was attributed to the characteristic peaks of hydroxy groups of n-HA [Fig. 1(b)], which moved to 3428 cm^{-1} in PAA/n-HA 30

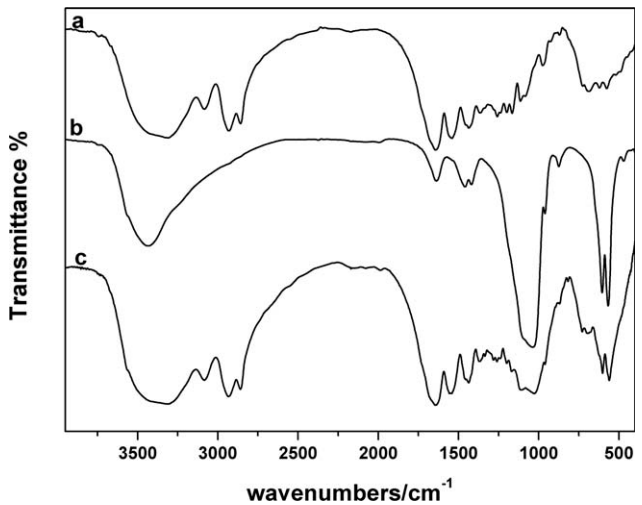

Figure 1 IR of (a) PAA, (b) n-HA, and (c) PAA/n-HA 30 composite.

composite [Fig. 1(c)]. The peaks at 1036 cm^{-1} and 566 cm^{-1} were assigned to the vibrations of PO_4^{3-} groups in n-HA [Fig. 1(b)], which decreased to 1033 cm^{-1} and 563 cm^{-1} in Figure 1(c). These transformations of characteristic absorption peaks might be caused from the interface interaction between n-HA and. Through the IR analysis, the peak positions of hydroxy groups (OH) and phosphate (PO_4^{3-}) groups of n-HA had some displacement in composites, showed combination between n-HA and PAA matrix.

XRD analysis

The XRD patterns of PAA, n-HA, and PAA/n-HA 30 composite were shown in Figure 2. The two peaks at $2\theta = 20.0°$ and 23.5° [Fig. 2(a)] were belonged to the characteristic diffraction pattern of PAA polymer, indicating that the PAA was semi-crystalline polymer. The characteristic peaks of n-HA appeared at $2\theta = 25.8°$, 31.7°, and 34.0° [Fig. 2(b)] in the PAA/n-HA 30 composite. The results revealed that the composite was composed of PAA and n-HA, and the synthesis of PAA/n-HA composite procedure did not change the nature of n-HA. Besides, the crystallinity of PAA decreased with the increase of n-HA content in the composite as shown in the Figure 2. The results also indicated that the presence of n-HA with enhanced crystal nucleation reduced the stereoregularity of the PAA and leaded to the formation of more disordered polymer crystals. As a result of n-HA crystals intercalating, the PAA into the PAA/n-HA composite shows lower crystallinity than pure PAA. The XRD analysis suggested that the PAA crystallinity decreased with the increase of n-HA content, which might be caused by the interaction between n-HA and PAA at their interface.

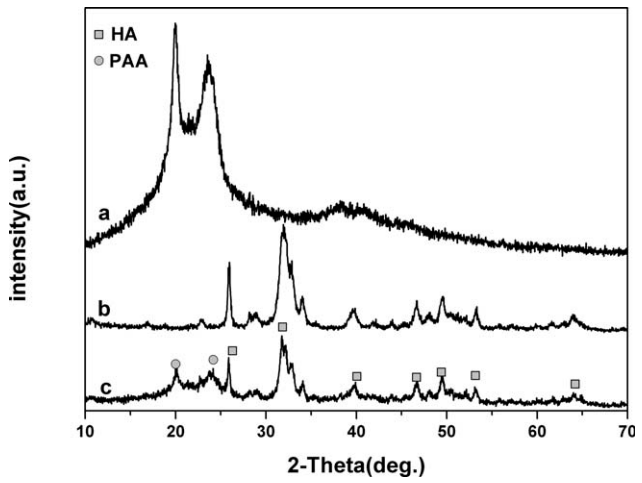

Figure 2 XRD of (a) PAA, (b) n-HA, and (c) PAA/n-HA 30 composite.

XPS analysis

XPS wide scan (Fig. 3) identified carbon, nitrogen, oxygen, calcium, and phosphor (from HA) as the major constituents of the PAA/n-HA composite. The binding energy of calcium atom (Ca), phosphorous atom (P), and oxygen atom (O) had some difference between n-HA (O1s: 530.9, Ca2p: 350.6 and 347.1, P2p: 133.0 eV) and the composite (O1s: 531.4, Ca2p: 351.6 and 348.0, P2p: 134.1 eV). The binding energy of O1s in the composite was higher than that of n-HA by 0.5, Ca by 1.0 and 0.9, and P by 1.1 eV respectively. The results indicated that chemical bonding was present between the n-HA and PAA.

Figure 4 showed the XPS Ca2p spectra, which had a doublet separated by $\sim$ 3.5 eV in binding energy for n-HA and PAA/n-HA composite. The Ca2p3/2 binding energy for n-HA was 347.1 eV and the Ca2p1/2 binding energy was 350.6 eV. The Ca2p3/2

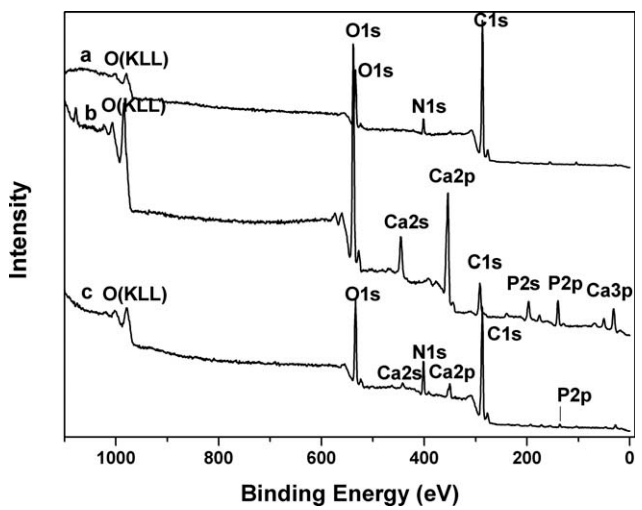

Figure 3 XPS curve of (a) PAA, (b) n-HA, and (c) PAA/n-HA 30 composite.

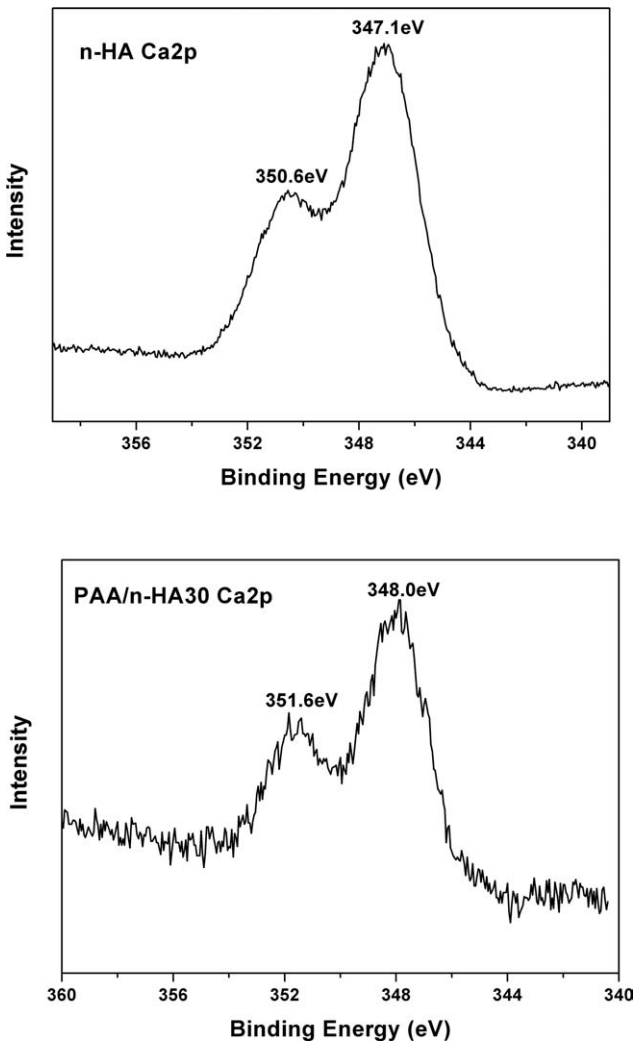

Figure 4 XPS Ca2p spectra of n-HA and PAA/n-HA 30 composite.

binding energy for PAA/n-HA composite was 348.0 eV and the Ca2p1/2 binding energy was 351.6 eV. It was clear that the binding energy of Ca2p for the composite was higher than that of n-HA by 1.0 eV. The XPS spectra showed us that in the composite the Ca^{2+} (form n-HA) was coordinated with both the PO_4^{3-} of n-HA and the $RCOO^-$ group of PAA molecule. Therefore, it could be deduced that n-HA bound with PAA by the formation of $RCOO^- \rightarrow Ca^{2+}$ linkage in the PAA/n-HA composite, which leaded to the increasing of the Ca2p binding energy in the composite. The binding energy of $RCOO^- \rightarrow Ca^{2+}$ bond was stronger than that of inorganic Ca^{2+}–PO_4^{3-} bond because the organic bond was with ionic and covalent properties.[20,21]

O1s binding energies at XPS spectra peak position (Fig. 5) were evaluated as 530.9, 531.9, and 531.4 eV for n-HA, PAA, and PAA/n-HA, respectively. The results showed that the O1s binding energy of the PAA/n-HA composite was lower than that of PAA by 0.5 eV but higher than that of HA by 0.5 eV. When Ca^{2+} was coordinated with $RCOO^-$, the bond C=O was weakened and the bond Ca–O was strengthened, so the binding energy of O1s for the composite was lower than that of PAA but higher than that of HA. It also indicated that the chemical environment of O atoms in the composite was to be similar.

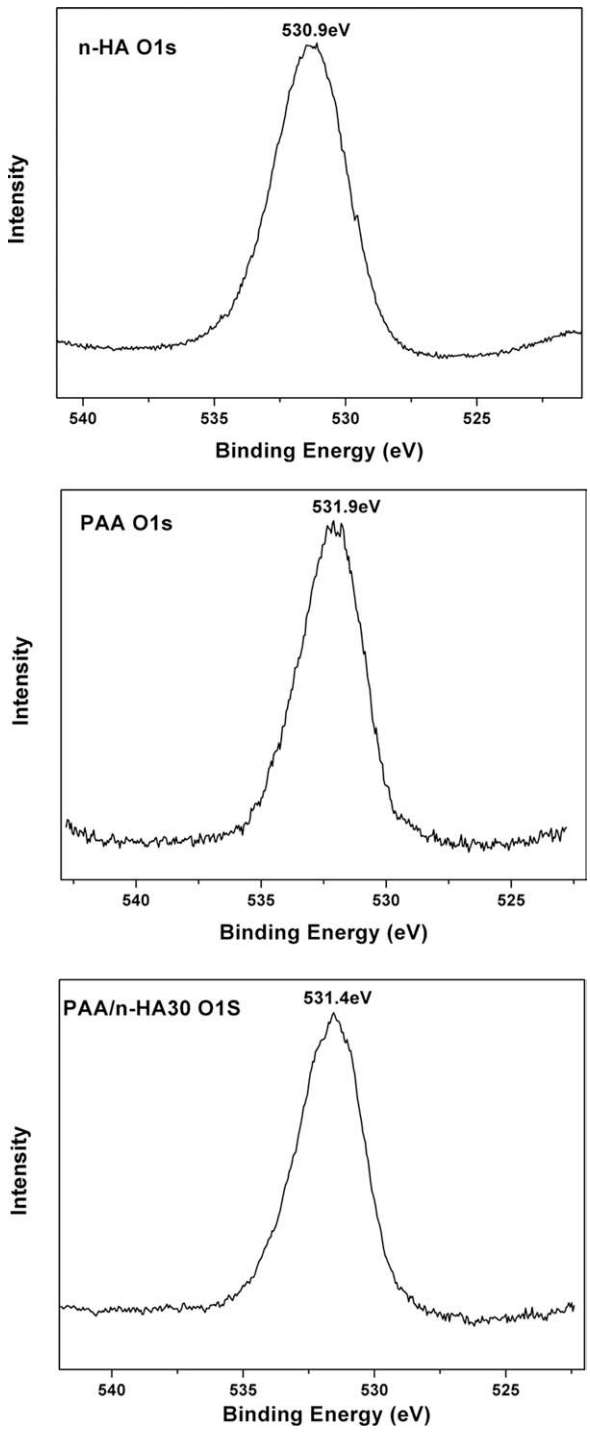

Figure 5 XPS O1s spectra of PAA, n-HA, and PAA/n-HA 30 composite,

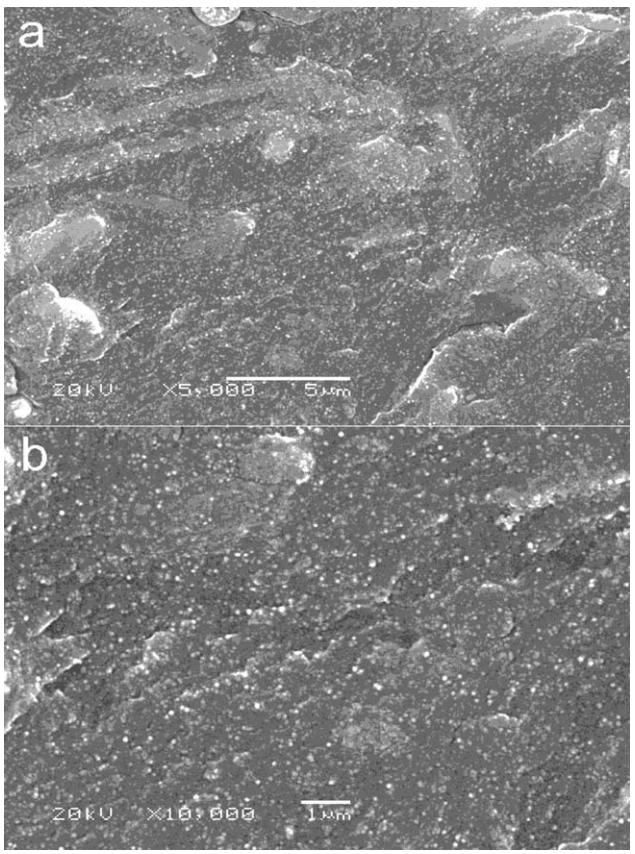

Figure 6 SEM images of surface morphology of PAA/n-HA 30 composite: (a) ×5000 and (b) ×10,000.

Overall, considering the results of IR, XRD, and XPS, it could be drawn a conclusion that strong interactions were present between the n-HA and PAA interface in the composite

Surface morphology

Figure 6 showed the SEM images of the surface morphology of the PAA/n-HA composite containing 30 wt % n-HA. The SEM examinations of different magnification revealed that n-HA particles with the size of about 80–100 nm were well dispersed in the polymer matrix. No obvious agglomeration of the n-HA particles was found in the PAA/n-HA composite. To improve the dispersion of n-HA into PAA matrix, an *in situ* melting polymerization method with a strong stirring was introduced into the synthetic process of PAA/n-HA composite. The poly(amino acid) polymers are considered to be promising biomedical materials because of their polypeptide backbone, which have the potential to be degraded into amino acid monomers in biological environments.[16] In addition, n-HA has excellent biocompatibility and bioactivity. Therefore, combination with the good properties of both PAA and n-HA, the bioactive composite of PAA and n-HA was designed and prepared in this study. The PAA/n-HA composite might have clinical potential for load-bearing bone repair or substitution.

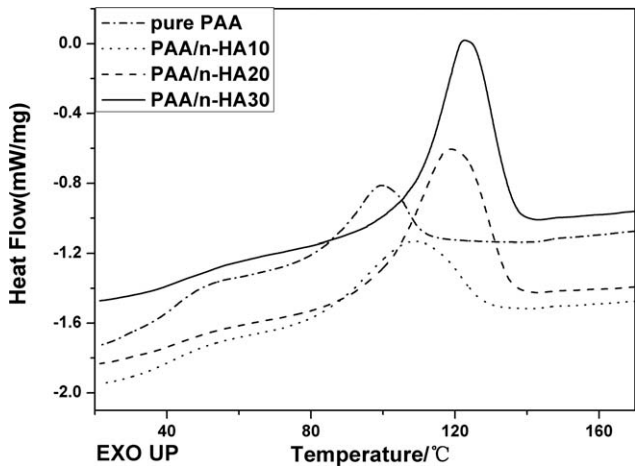

Figure 7 First cooling curves of PAA/n-HA composites with different HA content.

DSC analysis

The DSC curves of the PAA/n-HA composites with different n-HA content were shown in Figures 7 and 8. The results showed that the T_g of PAA/n-HA composites containing 0 wt %, 10 wt %, 20 wt %, 30 wt % of n-HA were 47.4°C, 49.4°C, 49.7°C, 50.3°C, respectively. Clearly, the T_g of the samples gradually increased with increment of n-HA. The reasons might be as follows: first, there existed interfacial interaction between PAA and n-HA. Second, the thermal motions of molecular chain segments of PAA were constrained by n-HA. The results indicated that the n-HA play an important role in the changes of T_g of the composites. As for a polymer, the T_g must be high enough to provide stable

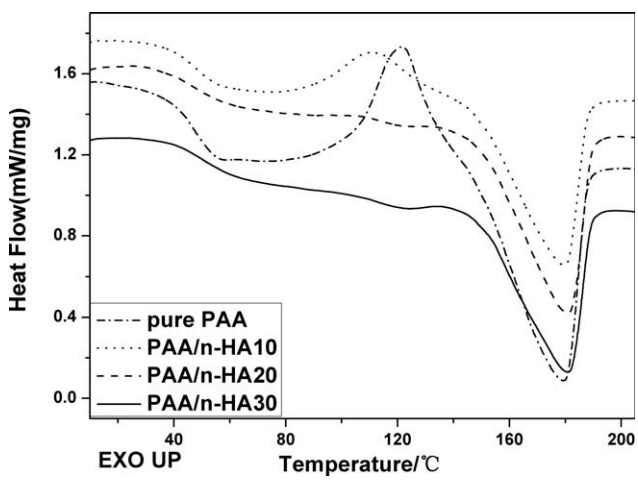

Figure 8 Second heating curves of PAA/n-HA composites with different HA content.

TABLE I
DSC of the PAA/n-HA Composites with Different Apatite Content

	T_g (°C)	T_{cc} (°C)	T_m (°C)	T_c (°C)
PAA	47.4	121.7	179.6	99.6
PAA/n-HA 10	49.4	110.3	179.4	109.8
PAA/n-HA 20	49.7	106.9	180.7	118.7
PAA/n-HA 30	50.3	–	180.9	122.6

T_g is glass transition temperature, T_{cc} is cold crystallization temperature, T_m is melting temperature, T_c is crystallization temperature.

structural rigidity during its applications. The T_g of the PAA/n-HA 30 composite was about 50.3°C, which suggested that the PAA/n-HA 30 composite had good suitability as used in biological systems, and the polymer based composite could also be easy shaped when it was used in repair irregular bone defects due to the low glass transition temperature.

In Table I, the cold-crystallization temperature (T_{cc}) as well as crystallization temperature (T_c), and the melting temperature (T_m) of the PAA/n-HA composites were represented. The crystallization temperature progressively increased whereas the cold crystallization temperature decreased with the increase of n-HA content, revealing that the n-HA was able to accelerate the crystallization of PAA by heterogeneous nucleation. Additionally, as for melting temperature, it increased with the increase of n-HA content. The results demonstrated that the n-HA content had obviously effects on the crystallization kinetic parameters and thermo properties of the PAA/n-HA composites.

Dynamic mechanical analysis

Dynamics mechanical analysis of PAA/n-HA composites with different n-HA content were performed to monitor the effects of n-HA on the thermomechanical properties of PAA. The storage modulus (E') of PAA/n-HA composites with various n-HA contents were plotted against temperature in Figure 9. The storage modulus E' was correlated with the elastic modulus of the materials. The value of E' reveals the capability of a material to store mechanical energy and resist deformation. The higher the storage modulus, the harder the material is.[22] From Figure 9, it was found that the storage modulus of the PAA/n-HA composites was significantly affected by the n-HA content. The addition of n-HA into the PAA matrix resulted in the increment of modulus of the PAA/n-HA composites, indicating that n-HA had a strong reinforcing effect on the elastic properties of PAA. The increase of E' of the composites with the increase of n-HA amount demonstrated that there was an interface interaction

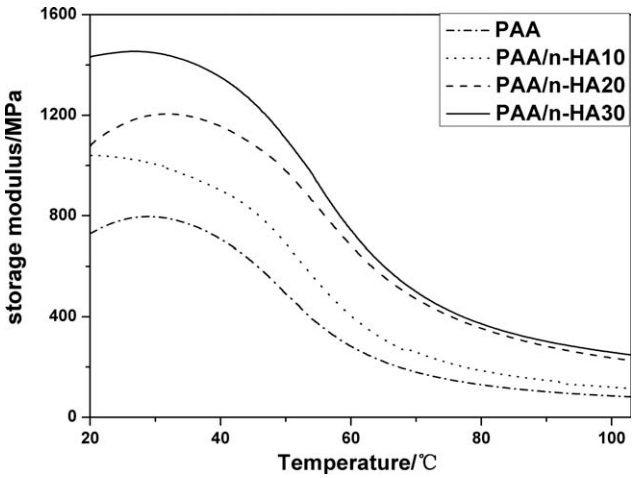

Figure 9 Storage modulus E' versus temperature of PAA/n-HA composites with different n-HA content.

between PAA and n-HA, which enhanced the chain packing and restricted the polymer molecular chain mobility at the interface of PAA and n-HA in the composite.[23,24]

The variation of the loss factors (tan δ) of the PAA/n-HA composites as a function of temperature were shown in Figure 10. The glass transition temperature was assigned as the temperature at peak maximum of tan δ in the DMA scan. Figure 7 showed that the T_g of PAA, PAA/n-HA 10, PAA/n-HA 20, and PAA/n-HA 30 composites were 59.2°C, 62.6°C, 63.8°C, 65.6°C, respectively. As mentioned earlier, the glass transition temperature of the PAA/n-HA composites increased with increase of n-HA content, this result was accorded with DSC analysis. Additionally, it was found from Figure 10 that the tan δ peak of the PAA/n-HA composites dropped with increase of n-HA content. The variation of the tan δ peak might be caused by the reason as follows: the addition of n-HA restricted the mobility of the

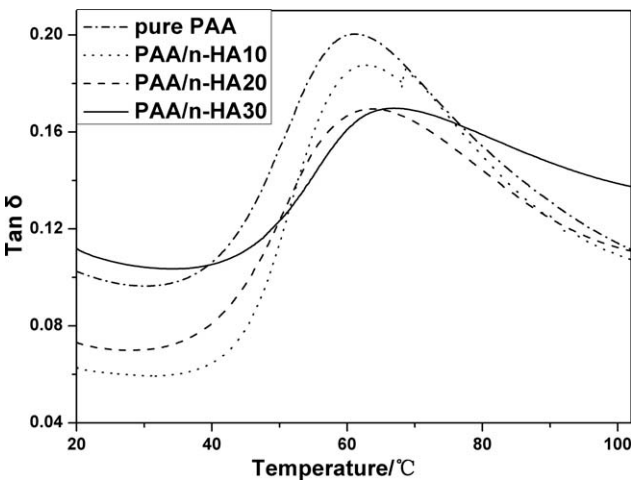

Figure 10 Loss factor tan δ versus temperature of PAA/n-HA composites with different HA content.

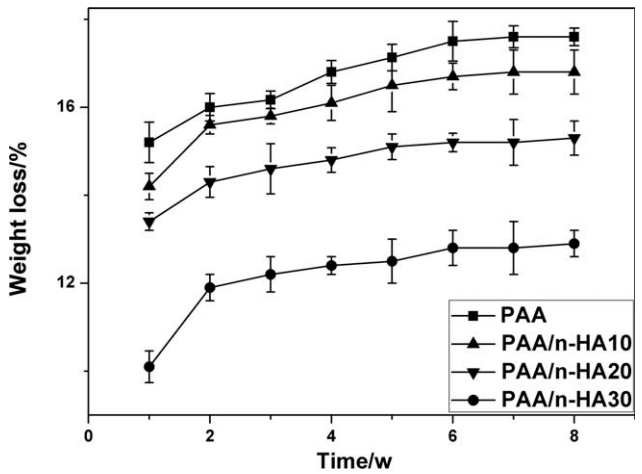

Figure 11 Weight loss of PAA/n-HA composites containing different HA content after immersion into PBS with time.

PAA polymer chains, and reduced the free volume in the composite, thus leading to the decrease of the intensity of the tan δ peak. The drops of tan δ demonstrated that there existed the interface interactions between the n-HA and PAA matrix.[24,25]

The results of DMA analysis of PAA/n-HA composites with different n-HA showed that the storage modulus of the composites increased while the intensity of tan δ peak decreased with the increase of n-HA content. This might be caused by the interface interaction existed between the n-HA and PAA, which enhanced the chain pack and restricted the polymer molecular chain mobility.

In vitro degradation of PAA/n-HA composite

Weight loss in PBS

Figure 11 displayed the weight loss ratio of the PAA, PAA/n-HA 10, PAA/n-HA 20, and PAA/n-HA 30 composites after immersion into PBS with time. It was found that there was a burst in weight loss for all the samples at the first week of incubation. After that, the weight loss of the composites decreased slowly with the soaking time for PAA/n-HA composites with different HA content. The results showed that the PAA degraded faster than the PAA/n-HA composites during the whole period, and the weight loss ratio of composites decreased with increasing content of n-HA.

After 8 weeks, it was found that the weight loss ratio of PAA, PAA/n-HA 10, PAA/n-HA 20, and PAA/n-HA 30 composites were 17.6%, 16.7%, 15.3%, and 13.0%, respectively. The reasons might be as follows: there existed interfacial interaction between PAA and n-HA when the PAA was filled with n-HA, which restricted water molecule to infiltrate into the composites, leading to the decrease of degradation ratio of the composites. In addition, the degradable ratio of HA was lower than PAA.

The results demonstrated that the amount of n-HA in the composites had obvious effects on the weight loss ratio of the PAA/n-HA composites. It was very important for the biomaterials with suitable degradation property when implanted in the physiological environment. The composites only degraded a portion during the soaking time, so the materials would not be to fail premature and can provide mechanical support at the initial stage of bone tissue repair.

pH value change of the soaking medium

The pH value variation of the medium after the samples soaking into PBS was shown in Figure 12. At the early stage of soaking (1 w), the pH of the incubation medium gradually decreased from 7.42 to 7.30, 7.31, and 7.33 for PAA/n-HA 10, PAA/n-HA 20, and PAA/n-HA 30 composites, respectively. In addition, the pH of the pure PAA decreased from 7.42 to 7.28 until 2 weeks. From the second week, it was found that the pH value for all the samples slowly increased, the pH value ultimately stabilized around 7.40.

As shown in Figure 11, the degradation rate of PAA in the PBS was faster than that of PAA/n-HA composites due to the presence of n-HA, the decrease of pH value was attributed to the degradation of PAA. During the period of incubating into the PBS, the poly(amino acid) degraded into amino acid monomers. The higher the degradation ratio, the lower the pH value was. Because the amino acid used in preparing the PAA polymer was acidic amino acid except lysine. The pH value of the physiological environment after biomaterials implanted *in vivo* would greatly influence cellular responses.[26]

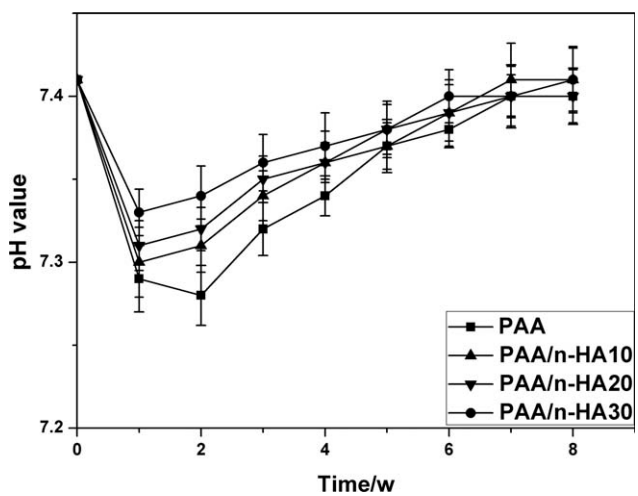

Figure 12 pH value change of PBS after PAA/n-HA composites containing different HA content soaking with time.

In this study, the results showed that the pH of the PBS solution decreased for PAA from 7.4 to 7.28 and for PAA/n-HA 30 from 7.4 to 7.33 at the first 2 weeks. With the soaking time prolonged, the pH values of the PBS solution for both PAA and PAA/n-HA composites increased slowly. The final pH value was stable around 7.40 for PAA and PAA/n-HA composites. The results indicated that both PAA and PAA/n-HA composites would not cause inflammatory response in physiological environment.

CONCLUSIONS

A bioactive composite of PAA/n-HA was prepared using the *in situ* melting polymerization method in the study. The reinforcing effect of n-HA into composite was confirmed by using the dynamic mechanical analysis, and the increase of storage modulus with the increase of n-HA content was detected. Additionally, There were some interaction at the interface between n-HA and PAA matrix, which would improve the mechanical performance of PAA/n-HA composite. The weight loss ratio of PAA/n-HA composite stabilized at 13.0% and the pH value of the medium was stable around 7.40 after immersion into the PBS for 8 weeks.

References

1. Johnson, A. J. W.; Herschler, B. A. Acta Biomater 2011, 7, 16.
2. Lee, S. J. J Ceram Process Res 2010, 11, 586.
3. Huang, H. Y.; Liu, Z. H.; Tao, F. Clin Neurol Neurosurg 1997, 99, 20.
4. Ahn, E. S.; Gleason, N. J.; Nakahira, A. Nano Lett 2001, 1, 149.
5. Yang, C.; Guo, Y. K.; Zhang, M. L. T Nonferr Metal Soc 2010, 20, 263.
6. Rezwan, K.; Chen, Q. Z.; Blaker, J. J Biomater 2006, 27, 3413.
7. Armentano, I.; Dottori, M.; Fortunati, E. Polym Degrad Stab 2010, 95, 2126.
8. Nejati, E.; Mirzadeh, H.; Zandi, M. Compos: Part A 2008, 39, 1589.
9. Peng, F.; Yu, X. H.; Wei, M. Acta Biomater 2011, 7, 2585.
10. Fukushima, K.; Abbate, C.; Tabuani, D. Polym Degrad Stab 2009, 94, 1646.
11. Buczynska, J.; Pamula, E.; Blazewicz, S. J Appl Polym Sci 2011, 121, 3702.
12. Kim, S. S.; Park, M. S.; Jeon, O. Biomaterials 2006, 27, 1399.
13. Zhao, J.; Guo, L.Y.; Yang, X. B. Appl Surf Sci 2008, 255, 2942.
14. Kim, S. Y. J Appl Polym Sci 2011, 121, 1921.
15. Martin, C.; Winet, H.; Bao, J. Y. Biomaterials 1996, 17, 2373.
16. Rypacek, F. Polym Degrad Stab 1998, 59, 345.
17. Sun, H.; Meng, F.; Dias, A. A. Biomacromolecules 2011, 12, 1937.
18. Yang, S. R.; Kim, S. B.; Joe, C. O. Biotechnol Lett 2005, 27, 977.
19. Yan, Y. G.; Li, H.; Lv, G. Y.; Cao, X.; Wang, Y. F.; Yang, A. P.; Luo, X. M.; Pei, H. X. Song, Y. M.; Duan, H. China patent No.101342384A, 2009.
20. Jie, W.; Li, Y. Eur Polym J 2004, 40, 509.
21. Chang, M. C.; Tanaka, J. Biomaterials 2002, 23, 3879.
22. Ni, J.; Wang, M. Mater Sci Eng C Biol Sci 2002, 20, 101.
23. Kwiatkowska, M.; Broza, G.; Schulte, K. Rev Adv Mater Sci 2006, 12, 154.
24. Cho, D.; Lee, S.; Yang, G. M. Macromol Mater Eng 2005, 290, 179.
25. Chou, W. J.; Wang, C. C.; Chen, C. Y. Compos Sci Technol 2008, 68, 2208.
26. Richert, L.; Arntz, Y.; Schaaf, P.; Voegel, J. C.; Picart, C. Surf Sci 2004, 570, 13.